Electronic Supplementary Material (ESI) for RSC Advances.

Supporting Information

Controlled Supramolecular Interaction to Enhance the Bioavailability of Hesperetin on Targeted Cancer Cells Through Graphyne: A Comprehensive in *Silico study*

Maroof Ahmad Khan[a], Javed Iqbal[*b], Mubashar Ilyas[b], Ali Raza Ayub[a], Yanhong Zhu[a], Hui Li[*a]

[a]*Key Laboratory of Clusters Science of Ministry of Education, School of Chemistry and Chemical Engineering, Beijing Institute of Technology, Beijing 100081, P.R.China.*

[b]*Department of Chemistry, University of Agriculture, Faisalabad-38000, Pakistan.*

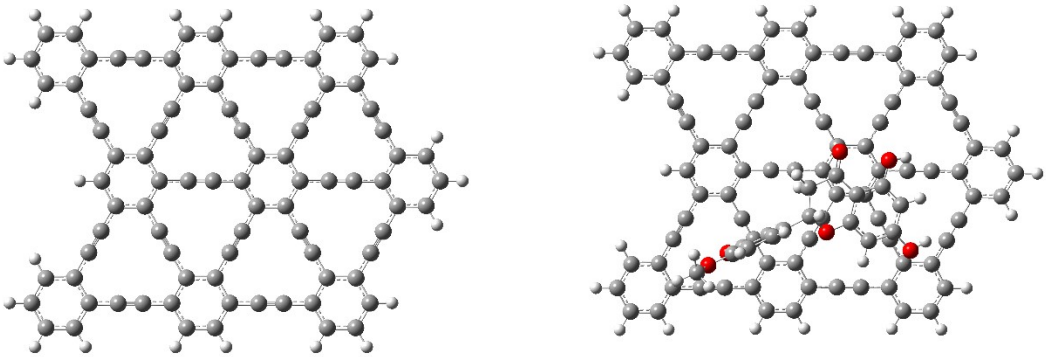

Figure S1. The optimized structure of GRP and HPT@GRP-complex in the aqueous phase.

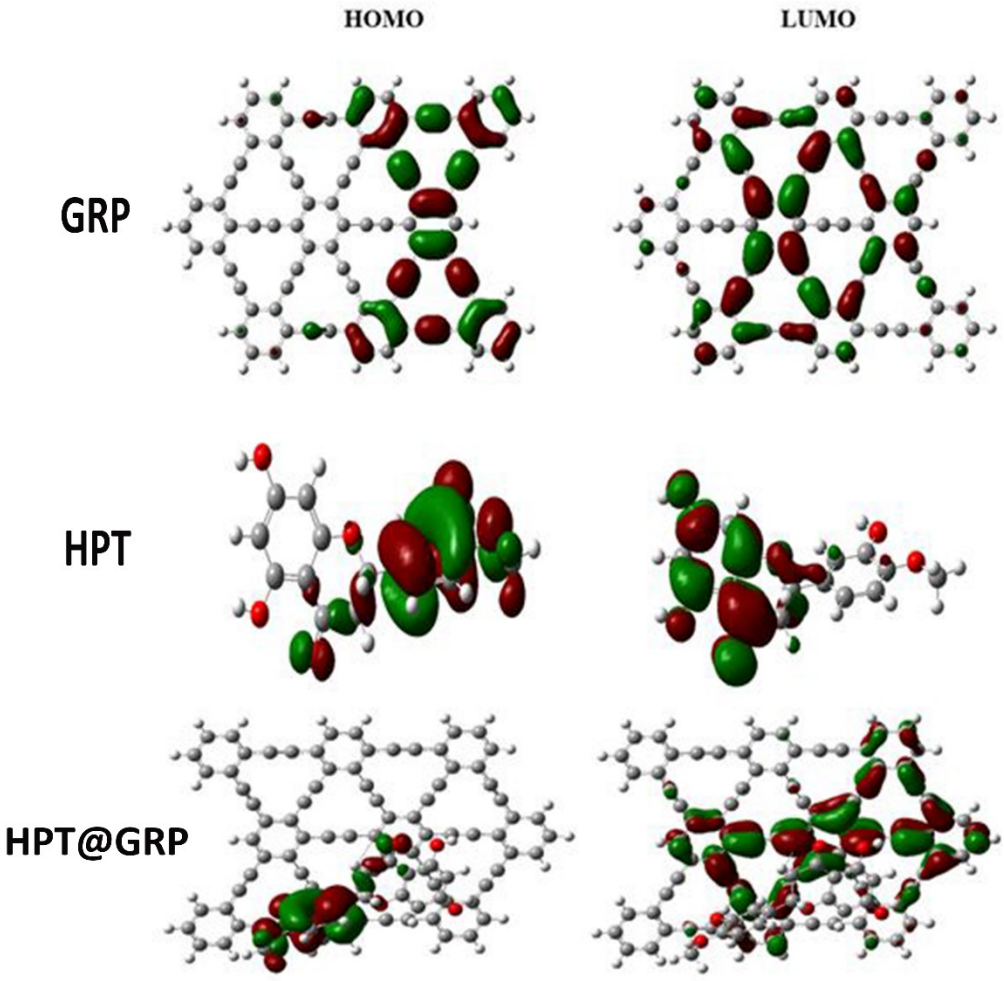

Figure S2. The HOMO-LUMO diagram of HPT, GRP and HPT@GRP-complex.

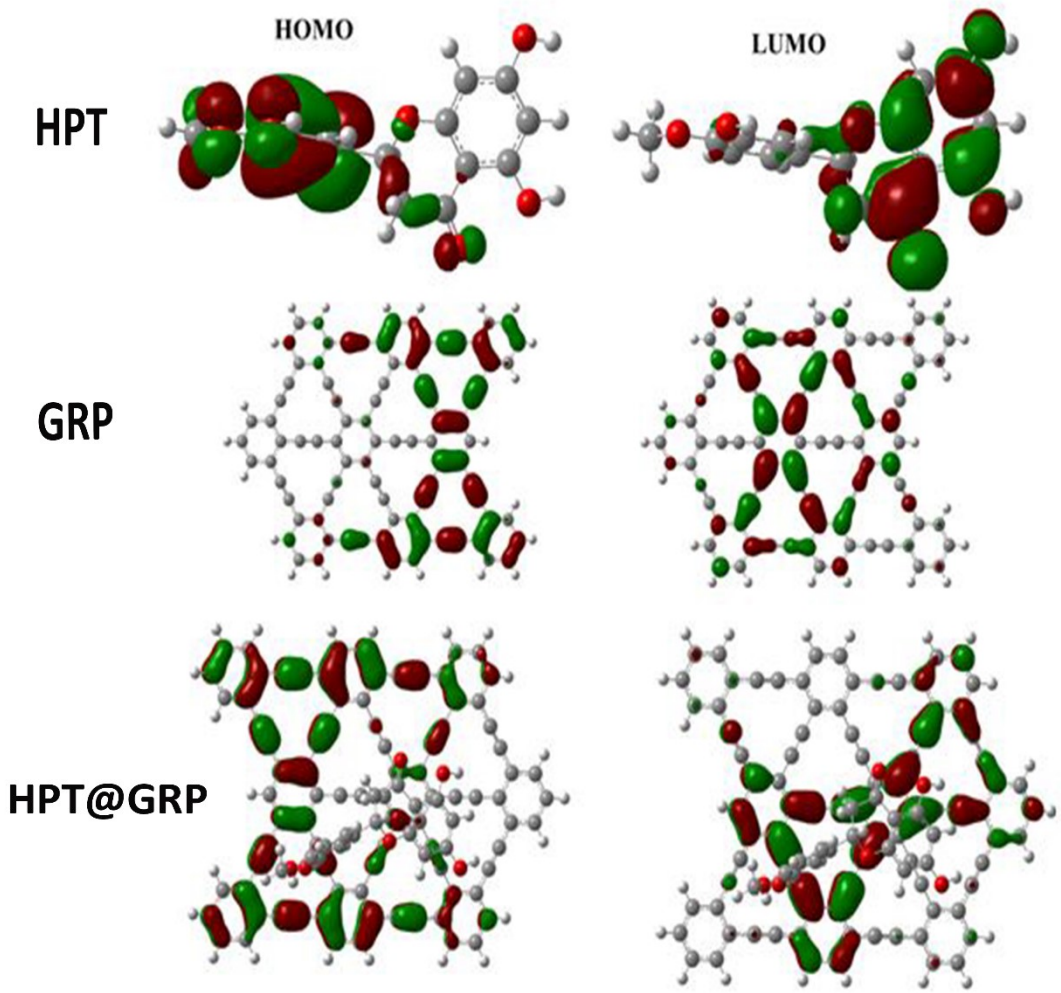

Figure S3. The HOMO-LUMO diagram of HPT, GRP and HPT@GRP-complex.

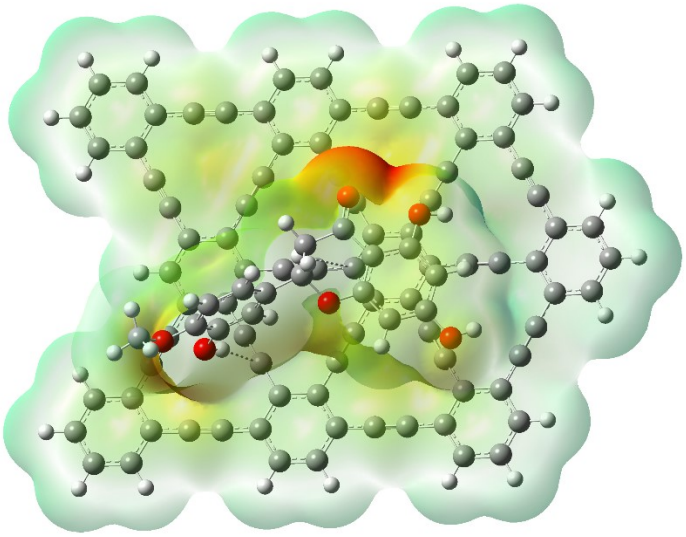

Figure S4. The MEP diagram of HPT@GRP-complex in an aqueous phase.

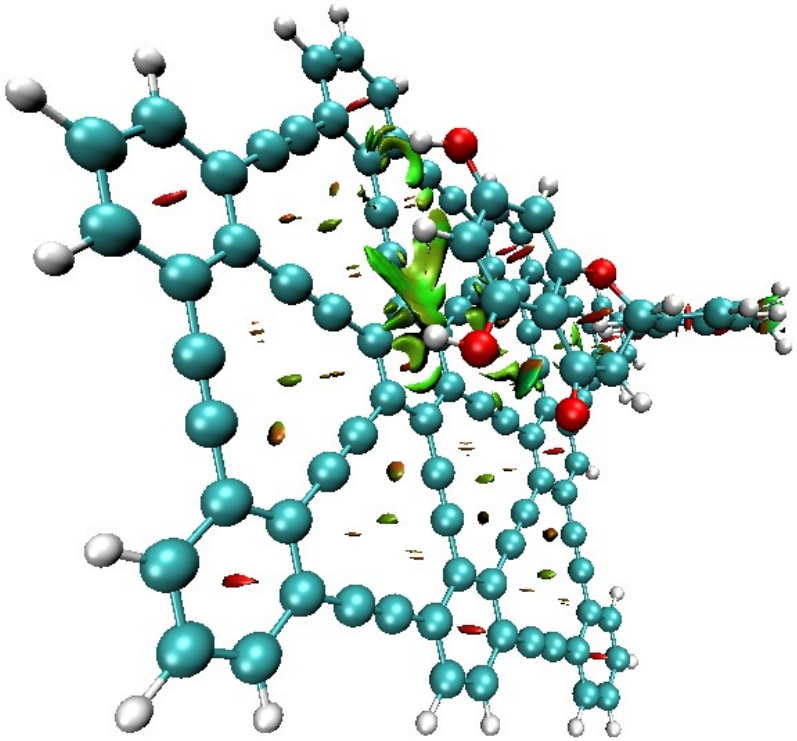

Figure S5. 3D color-filled iso-surface image of HPT@GRP complex.

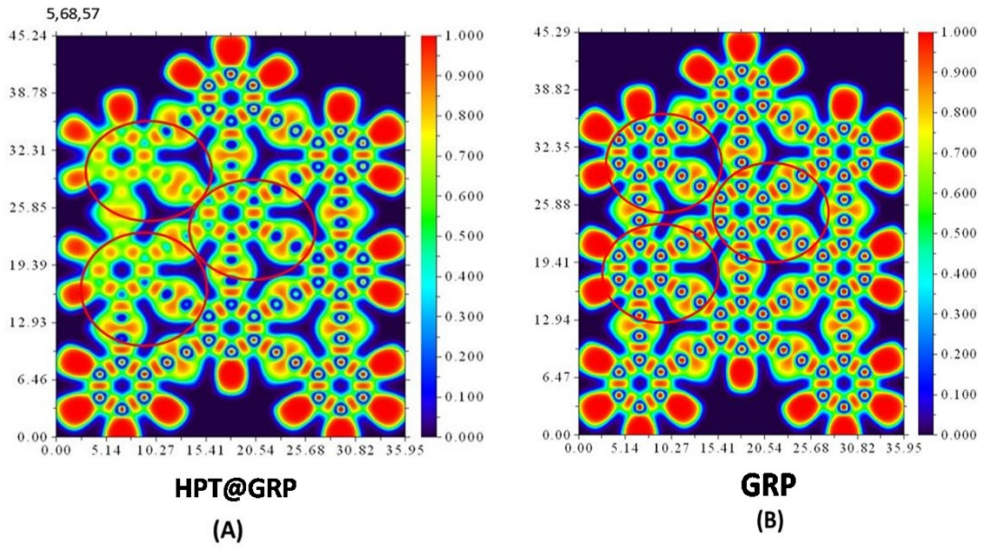

Figure S6. Electron-density plots (A) ELF image for the GRP present in the HPT@GRP complex (B) ELF image for GRP.

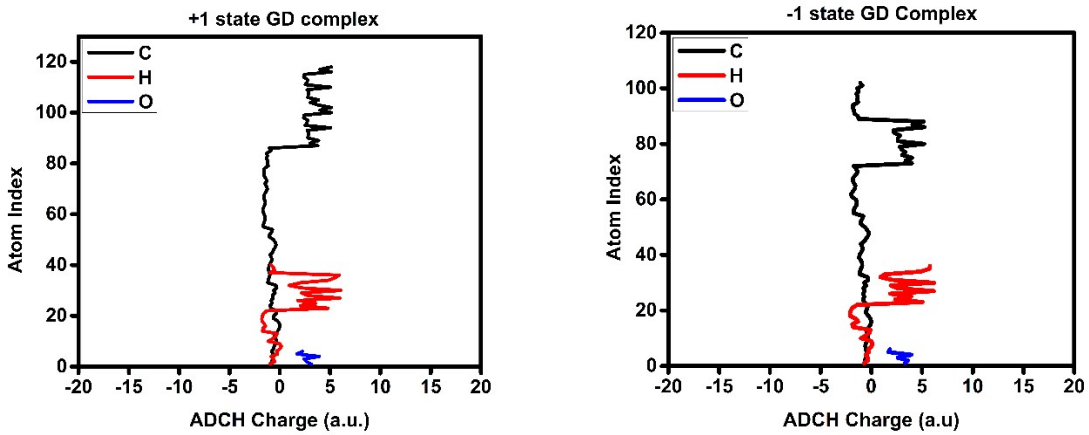

Figure S7. The ADCH charges for *HPT@GRP*$^{-1/+1}$ complexes.

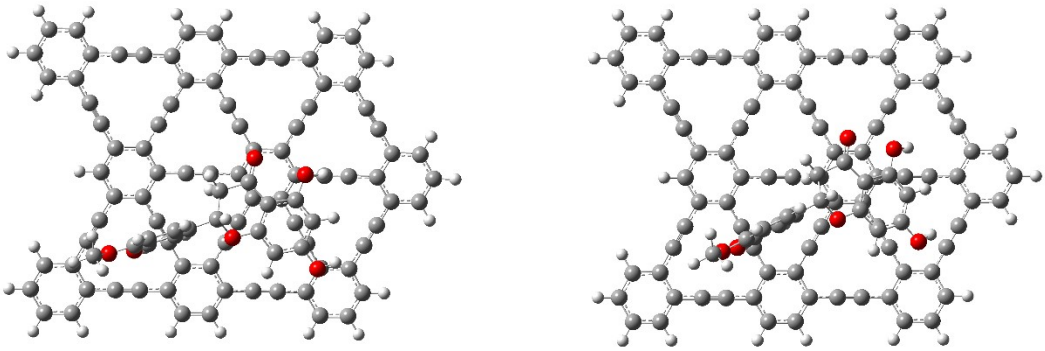

Figure S8. The optimized structure of HPT@GRP^{+1}complex and HPT@GRP^{-1}complex.

Table S1. The HOMO-LUMO and chemical descriptors include vertical ionization energy, vertical electron affinity, and dipole moment in the aqueous phase.

Parameters	HPT	GRP	HPT@GRP
E_{HOMO} (eV)	-5.74	-5.80	-5.58
E_{LUMO} (eV)	-1.29	-3.24	-3.07
ΔE (eV)	4.447	2.56	2.51
VIP (eV)	5.74	5.80	5.58
VEA (eV)	1.29	3.24	3.07
η (eV)	2.223	1.28	1.25
μ (eV)	-3.51	-4.52	-4.32
X (eV)	3.51	4.52	4.32
σ	0.224	0.39	0.40
ω (eV)	2.77	7.98	7.46
Dipole moment	4.13D	0.47D	3.55D
λmax	200.14	520.96	525.93

Table S2. The I.R. spectrum information of HPT, GRP, and HPT@GRP-complex.

HPT@GRP	HPT	GRP	vibration	Effects	Comments
3839.87	3821.84	x	v_sO5-H32	Blueshift	Hydrogen bonding
3184.01	3011.76	x	v_sC22-H36	Blueshift	Hydrogen bonding
3259.21	x	3259.21	v_sC15-H18	No shift	No significant effect observed
2401.10	x	2401.21	v_sC29-C28	No shift	No significant effect observed
3257.04	x	3256.95	v_sC15-H18	Blueshift	Van der Waals forces
3058.25	3012.53	x	v_s C22-H36	Blueshift	Van der Waals forces
3175.56	3073.38	x	v_s C8-H25	Blueshift	Van der Waals forces
779.32	752.51	x	β_{as}C12-O1-C7	Blueshift	Week forces + Hydrogen bonding
952.36	x	953.48	β_s C56-C57-C58	redshift	Van der Waals forces
981.58	x	1023.82	β_{as}C95-C96-C71	redshift	Van der Waals forces

Table S3. ELF (electron-localization function) and NBO analysis

GRP → GRP	
Mode of Transition	kcal/mol
$\pi_{C66-C67} \rightarrow \sigma^*_{C126-C137}$	0.15
$\pi_{C101-C102} \rightarrow \pi^*_{C126-C127}$	0.13
$\pi_{C50-C51} \rightarrow \pi^*_{C118-C123}$	0.12
$\pi_{C64-C65} \rightarrow \sigma^*_{C116-C132}$	0.12
$\pi_{C66-C67} \rightarrow \pi^*_{C126-C127}$	0.11
$\pi_{C66-C67} \rightarrow \sigma^*_{C111-C139}$	0.09
$\pi_{C105-C106} \rightarrow \sigma^*_{C121-C134}$	0.08
$\pi_{C50-C51} \rightarrow \pi^*_{C126-C127}$	0.06
HPT → GRP	
Mode of Transition	kcal/mol
LP (2) $_{O114} \rightarrow \pi^*_{C101-C102}$	0.15
$\pi_{C126-C127} \rightarrow \pi^*_{C101-C102}$	0.07
LP $(2)_{O111} \rightarrow \pi^*_{C52-C53}$	0.07
LP $(2)_{O113} \rightarrow \pi^*_{C105-C106}$	0.06
$\pi_{C126-C127} \rightarrow \pi^*_{C66-C67}$	0.05
Energy change before and after adsorption	
Mode of Transition	Before kcal/mol **A**fter kcal/mol
$\pi_{C22-C23} \rightarrow \pi^*_{C20-C21}$	20.67 20.88
$\pi_{C57-C58} \rightarrow \pi^*_{C55-C56}$	20.7 20.88
$\pi_{C45-C46} \rightarrow \pi^*_{C43-C44}$	20.24 20.76
$\pi_{C82-C83} \rightarrow \pi^*_{C80-C81}$	20.23 20.4
$\pi_{C4-C5} \rightarrow \pi^*_{C1-C6}$	19.5 19.46
$\pi_{C1-C6} \rightarrow \pi^*_{C2-C3}$	19.42 19.4
$\pi_{C66-C67} \rightarrow \pi^*_{C59-C60}$	13.13 13.06
$\pi_{C28-C29} \rightarrow \pi^*_{C2-C3}$	12.58 12.65
$\pi_{C97-C98} \rightarrow \pi^*_{C70-C71}$	12.39 12.58
$\pi_{C412-C59} \rightarrow \pi^*_{C40-C41}$	11.82 11.76